Stretched-Pulse Soliton Kerr Resonators

Xue Dong,* Qian Yang, Christopher Spiess, Victor G. Bucklew, and William H. Renninger
Institute of optics, University of Rochester, Rochester, New York 14627, USA

(Received 28 February 2020; revised 15 May 2020; accepted 12 June 2020; published 17 July 2020)

Kerr resonators support novel nonlinear wave phenomena including technologically important optical solitons. Fiber Kerr resonator solitons enable wavelength and repetition-rate versatile femtosecond-pulse and frequency-comb generation. However, key performance parameters, such as pulse duration, lag behind those from traditional mode-locked laser-based sources. Here we present new pulse generation in dispersion-managed Kerr resonators based on stretched-pulse solitons, which support the shortest pulses to date from a fiber Kerr resonator. In contrast to established Kerr resonator solitons, stretched-pulse solitons feature Gaussian temporal profiles that stretch and compress each round trip. Experimental results are in excellent agreement with numerical simulations. The dependence on dispersion and drive power are detailed theoretically and experimentally and design guidelines are presented for optimizing performance. Kerr resonator stretched-pulse solitons represent a new stable nonlinear waveform and a promising technique for femtosecond pulse generation.

DOI: 10.1103/PhysRevLett.125.033902

Kerr resonators are one of the simplest systems supporting complex nonlinear optical phenomena. They have attracted considerable attention recently for their practical value in generating ultrashort optical pulses and frequency combs. Frequency combs are desirable for several applications, including spectroscopy, frequency synthesis, distance ranging, attosecond pulse generation, as well as astronomical spectrograph calibration [1–9]. Kerr resonators can be made very compact, including on chip [10,11] for frequency-comb generation with a small form factor, simple processing, low drive powers, as well as gigahertz to terahertz line spacing [12,13]. At the macroscale, in bulk Kerr enhancement cavities, reduced nonlinear material enables new performance for pulse compression at much higher energy levels [14]. The earliest demonstrations of Kerr resonator pulse generation were in fiber-based cavities, with sizes in between the micro and bulk regimes [15]. Initial demonstrations in fiber were motivated by all-optical buffering [15,16], and more recent research illustrates fascinating long-range interactions [17], spatiotemporal instabilities [18], and a new platform for temporal tweezing [19]. In comparison with other Kerr resonator platforms, fiber offers excellent thermal management, strict single-mode operation, very low waveguide loss, and commercially available high-quality optical components.

Kerr resonators are driven by a continuous-wave laser and generate a broad bandwidth of cavity modes through parametric frequency conversion. To establish temporal coherence and a regular phase relationship between the cavity modes, the Kerr resonator must be mode locked. As with laser systems with an active gain medium, Kerr resonators are mode locked through the formation of optical solitons in the cavity [20,21]. The most common soliton-mode locking in Kerr resonators is related to that in laser systems: the pulse is formed through a balance between the effects of anomalous group-velocity dispersion (GVD) and the Kerr nonlinear phase, with a subtle difference in the pulse parameters [22,23]. However, while related, the difference between a broadband laser gain and the single-frequency drive in Kerr resonators is highly nontrivial and important questions are unanswered. For example, could the advanced soliton techniques used for mode-locking lasers be applicable to Kerr resonators as well? While Kerr resonators can support wavelength and repetition-rate versatile pulses, the duration of these pulses is much longer than that from mode-locked lasers. This limitation may be avoided if the novel mode-locking techniques from lasers could be applied to Kerr resonators.

Stretched-pulse mode locking enables shorter femtosecond pulses to be generated from dispersion-managed lasers than from soliton mode locking in all-anomalous dispersion lasers [24–27]. The pulses stretch and compress while traversing the cavity, reaching a Fourier-transform-limited duration twice per round trip. The pulses in these systems also feature a Gaussian profile, in contrast to the hyperbolic secant shape observed in anomalous dispersion systems. Stretched-pulse mode locking is now a common technique for mode-locking laser systems because it enables the shortest pulses from these systems, with durations now reaching a few optical cycles [24]. For Kerr resonators, while some progress has been made, stretched-pulse mode locking has not been demonstrated to date. Stretched-pulse solitons have been analyzed theoretically [28] and dispersion-managed Kerr resonators have been investigated experimentally with a focus on mechanisms for temporal binding [29] and the emission of

resonant radiation [30], but only a single spectral measurement corresponding to longer pulses is observed.

Here we report on the observation and analysis of stretched-pulse solitons in Kerr resonators. In strongly driven dispersion-managed fiber resonators with small and anomalous total dispersion, stable stretched-pulse solitons are generated. The pulses feature a broad spectral bandwidth and a compressed pulse duration of 210 fs, which is the shortest pulse duration observed to date from a fiber Kerr resonator. Numerical simulations, in agreement with experiments, reveal that the pulses stretch and compress twice per round trip in the cavity, with an overall stretching ratio that is larger than three. The pulse and spectral intensity are well fit to Gaussian profiles as they are in stretched-pulse mode-locked fiber lasers. The transform-limited pulse duration is strongly dependent on the total cavity dispersion and drive power. Improved performance is anticipated with larger drive powers and by compensating for the residual higher order dispersion. Stretched-pulse mode locking is a promising new technique for generating femtosecond pulses from fiber Kerr resonators, and may be applicable to other important platforms, including microresonators and bulk enhancement cavities.

Stretched-pulse soliton generation can be investigated theoretically using finite-difference time-domain numerical simulations. The cavity consists of one segment of anomalous (−) GVD fiber, one segment of normal (+) GVD fiber, an external drive, and additional fiber component losses [Fig. 1(a)]. The fiber sections are modeled with a nonlinear Schrödinger equation with parameters corresponding to commercially available fibers. The external drive and coupler losses are implemented as discrete elements one time per round trip (see Supplemental Material [31]). The choice of fiber lengths is instructed by related stretched-pulse laser cavities and modified until the desired operation is obtained (see Supplemental Material [31]). Stable representative stretched-pulse solitons are obtained in a cavity featuring a total dispersion that is slightly anomalous. The pulse energy converges to a steady-state value in fewer than 500 round trips [Fig. 1(b)]. The temporal and spectral intensity profiles [Figs. 1(c) and 1(d)] and the time-bandwidth product correspond well to a Gaussian profile, in contrast to the hyperbolic secant profiles characteristic of Kerr resonator solitons. The spectral bandwidth is 18-nm broad and changes minimally within the cavity, indicating the propagation is dominated by linear dispersive effects [28]. The pulse duration stretches and compresses twice per round trip in the cavity, with a maximum chirped pulse duration of 660 fs and a minimum dechirped duration of 210 fs [Fig. 1(a)]. This corresponds to a stretching ratio of > 3. This large intracavity evolution illustrates that the nonlinearity and dispersion are not balanced locally throughout the resonator, in contrast to traditional Kerr resonator solitons in anomalous dispersion cavities. However, the effects of the

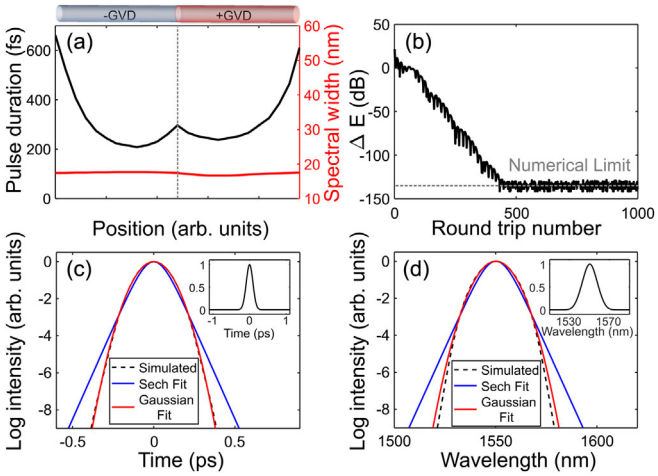

FIG. 1. Numerical simulations of stretched-pulse solitons. (a) Steady-state evolution of the pulse duration (black) and spectral bandwidth (red) in the −GVD and +GVD segments of one cavity round trip. Note that while the total dispersion of each fiber is nearly the same, the GVD and lengths differ (see Supplemental Material [31]). (b) Pulse convergence represented by the energy difference between pulses of successive round trips. (c) The log-scale simulated temporal intensity of the pulse when it is shortest with Gaussian (red) and hyperbolic secant (blue) fits. The linear-scale pulse is inset. (d) The corresponding log-scale simulated spectral intensity and Gaussian (red) and hyperbolic secant (blue) fits. The linear-scale spectrum is inset.

total dispersion, nonlinearity, as well as the drive and loss balance overall such that the evolution repeats every round trip.

Guided by the results of the numerical simulations, a fiber cavity was designed to generate stretched-pulse solitons experimentally (Fig. 2 and Supplemental Material [31]). The dispersion-managed cavity consists of two commercially available fibers with opposite signs of GVD (SMF28 with $\beta_2 = -22942$ fs^2/m and Metrocor with $\beta_2 = 9687$ fs^2/m)

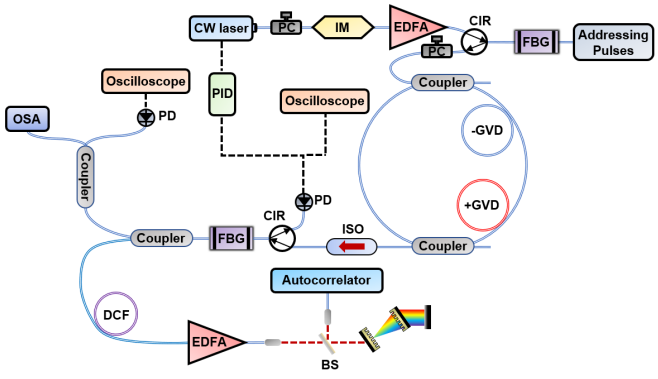

FIG. 2. Schematic of the experimental setup. Intensity modulator (IM), erbium-doped fiber amplifier (EDFA), fiber Bragg grating (FBG), optical spectrum analyzer (OSA), dispersion compensating fiber (DCF), polarization controller (PC), isolator (ISO), circulator (CIR), and beam splitter (BS).

and a total length of 7 m that is arranged such that the total magnitude of dispersion is small and anomalous (-4500 fs^2). The 1550-nm drive is comprised of a narrow-linewidth tunable laser that is intensity modulated into a train of 10-ns pulses matched to the 28.8 MHz repetition rate of the cavity and amplified by an erbium-doped amplifier [18,32,33]. The peak power of the pump is enhanced to a maximum of 5.1 W before it is input into the cavity through a 5% coupler. A fiber-Bragg grating filter is applied to the amplified drive to remove any unwanted amplified spontaneous emission from the amplifier. The polarization of the drive is adjusted with a fiber-format polarization controller to align with one of the principal polarizations of the cavity. The drive frequency is controlled piezoelectrically by the output of a proportional-integral-derivative (PID) control circuit using the cavity output power as an error signal. In this way, the cavity detuning can be controlled through the offset setting of the PID circuit. The cavity is addressed by an all-normal dispersion fiber laser with 8.2-MHz repetition rate and pulses with a 1-nm spectral bandwidth (see Supplemental Material [31]). These optical pulses periodically excite soliton formation through cross-phase modulation, as in previous fiber Kerr resonator studies [15,29]. After the 2% output coupler from the cavity, an additional fiber filter is used to filter out most of the residual continuous-wave drive light from the pulsed output. The filtered output spectrum is measured with an optical spectrum analyzer and the pulse train is measured with a photodiode and oscilloscope. Before the temporal autocorrelator, a commercially available normal dispersion fiber with negative third-order dispersion (TOD) is used to reduce the residual third-order dispersion from the fiber cavity and the pulses are amplified with an erbium-doped fiber amplifier. A grating pair is used to remove the residual group-velocity dispersion (chirp) from the output pulses.

By scanning through available settings for the drive power, polarization, frequency, and pump period, stable reproducible stretched-pulse solitons are observed experimentally [Fig. 3(a)–3(c)]. The output spectrum has a 3-dB bandwidth of ∼16 nm, with a small residual signature from the drive at the center frequency [Fig. 3(a)]. The pulse is analyzed with a two-photon autocorrelator as a function of the dispersion applied by a grating-pair compressor [Figs. 3(b)–3(c)]. The minimum compressed pulse duration corresponds to a pulse with a duration of 210 fs. This is the shortest pulse observed to date from a fiber Kerr resonator. The pulse duration varies smoothly as a function of the grating pair spacing, indicating coherence and a regular temporal phase [Fig. 3(c)]. The experimental results are reproduced with numerical simulations using matching parameter values. The simulations differ from those in Fig. 1 by including additional third-order dispersion consistent with experiments. Third-order dispersion has the effect of slightly reducing the half-max bandwidth from 18 to 16 nm as well as introducing a resonant radiation sideband at 1520 nm [Fig. 3(d)]. The energy of the pulse

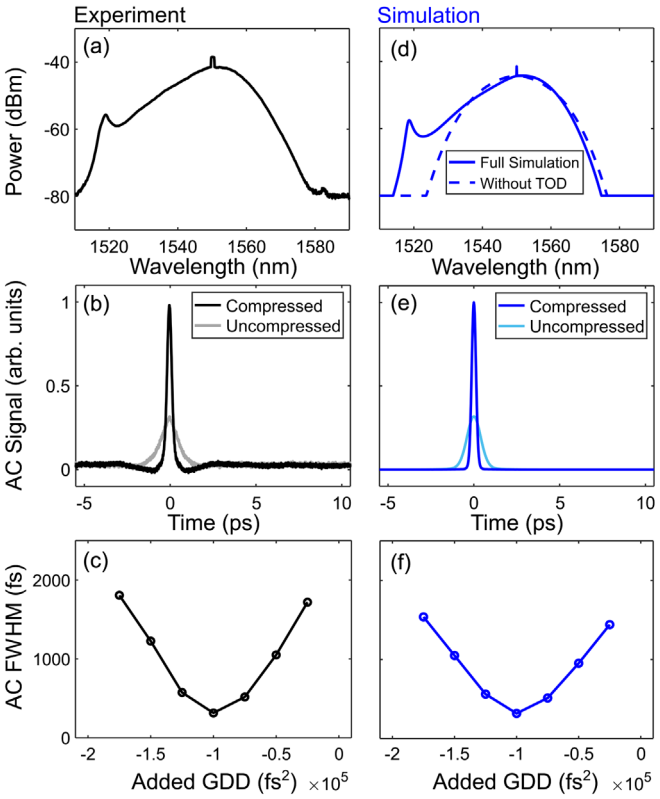

FIG. 3. Experimental (a) spectrum, (b) uncompressed output (gray) and compressed output (black) autocorrelation, and (c) autocorrelation duration as a function of the grating-pair group delay dispersion (GDD). Corresponding simulated (d) spectrum (solid), (e) uncompressed output (light blue) and compressed output (blue) autocorrelation, and (f) autocorrelation duration as a function of the grating-pair dispersion applied. The spectrum from simulations without TOD is plotted with a blue dashed line in (d) for comparison. Autocorrelation (AC) and full width at half the maximum (FWHM).

in the cavity, in agreement with simulations, is measured to be ∼13 pJ. The overall agreement between theory and experiment is excellent for this highly nonlinear system.

The dependence of stretched-pulses solitons on key system parameters is analyzed theoretically and experimentally. The bandwidth of the stretched-pulse solitons has a strong dependence on the net dispersion of the cavity. Experimentally, when the cavity has large net anomalous dispersion, it supports traditional solitons that do not stretch. When the cavity dispersion increases toward zero with the total length held constant, the bandwidth and stretching ratio increase. The broadest spectrum observed experimentally for each value of dispersion is shown in Fig. 4(a), with the corresponding bandwidth indicated by a point in Fig. 4(b). TOD-induced asymmetry is more pronounced when the net group-velocity dispersion is closer to zero. The spectral bandwidth increases inversely with the net dispersion, with the maximum bandwidth obtained close to zero. As the bandwidth increases, the stretching ratio increases until qualitative changes occur in

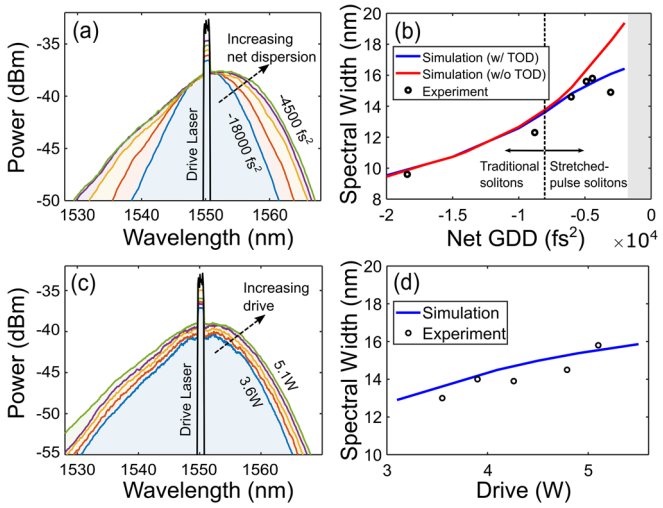

FIG. 4. Stretched-pulse soliton dependence on dispersion and drive power. (a) Broadest measured spectrum as a function of net group delay dispersion of the cavity. The drive laser frequency is plotted in black. (b) The broadest spectral bandwidth vs net dispersion from experiments (points) and simulations with (red line) and without (blue line) TOD. The black dashed line indicates the approximate minimum stretching ratio (2) corresponding to stretched-pulse solitons. More complicated behavior is found in the gray shaded region. (c) Broadest measured spectrum as a function of drive power. The drive laser frequency is plotted in black. (d) The broadest spectral bandwidth vs drive power from experiments (points) and corresponding simulations (blue line).

the stretched-pulse soliton regime with stretching ratios greater than 2. The experimental trends are compared to the results from numerical simulations with and without TOD [Fig. 4(b)]. TOD has the effect of decreasing the maximum supported bandwidth near zero net dispersion. Very close to zero net dispersion, distinct solutions are observed. Near zero dispersion, the solutions feature spectral bandwidths below 10 nm, stretching ratios larger than six, and prominent side lobe features in the time and spectral domains. This more complicated behavior near zero dispersion may be a subject of interest for future investigations. The spectral bandwidth also has a noticeable dependence on the power of the drive [Figs. 4(c) and 4(d)]. The spectral bandwidth varies linearly with the drive power with a slope in this case of ∼1 nm/W.

The dependence of stretched-pulse solitons on dispersion and drive power suggests opportunities for improved performance. Focusing on reducing the pulse duration (increasing the bandwidth), improvements can be made separately for the drive and the dispersion. The experimentally observed spectra are well matched to the broadest bandwidth spectrum obtained as a function of dispersion in the cavity. However, this is assuming the TOD of typical commercial fibers. If the higher-order dispersion can be removed or compensated, from Fig. 4(b), the bandwidth dependence could be exponential, allowing for broader bandwidths. The bandwidth is also limited by the maximum drive power currently available. The drive power can be improved in three ways. First, a higher power amplifier could be used. This, however, will introduce new average-power damage issues and is not preferable. The other two ways are enabled by the pulsed drive technique. The drive power is determined by the peak power of the drive pulses after amplification. This peak power scales inversely with the duty cycle of the pulses, which can be improved by either shortening the pulses or increasing the period of the pulses. The pulses can be shortened using higher frequency control electronics. 100-ps pulses, and a corresponding 2 orders of magnitude higher drive powers should be achievable in this way. The period can also be increased, but since this period must match that of the cavity, it will require an increase in the cavity length. However, increasing the length of the fiber increases the effect of Raman scattering, which is known to limit the performance of Kerr solitons [34]. Further studies are needed on the dependence of stretched-pulse soliton Kerr resonators on Raman scattering.

Stable stretched-pulsed soliton generation requires a drive laser that is locked to the resonance frequency of the cavity. This resonance is subject to environmental perturbations including from vibrations and temperature changes. The present resonator is not isolated from environmental perturbations. In addition, the drive period is freely running with respect to the cavity period which results in the solitons eventually becoming out of temporal alignment with the drive. From these combined effects the solitons are present for several minutes before needing to be readdressed. Environmental isolation, improved frequency locking, and locking the drive pulse period to the cavity period will significantly improve the lifetime of the solitons.

In this work we have presented experimental and theoretical observations of stretched-pulse Kerr solitons. In dispersion-managed fiber resonators, stretched-pulse solitons are observed, characterized by Gaussian spectral and temporal profiles and temporal stretching ratios greater than 3. The bandwidth, and corresponding transform-limited duration, is found to depend strongly on the drive power and the dispersion of the cavity. By optimizing these parameters, 210-fs pulses are observed, which corresponds to the shortest pulses observed to date from fiber Kerr resonators. With modest improvements to the drive and dispersion the performance is expected to improve further. Stretched-pulse Kerr resonators represent a promising new technique for femtosecond pulse generation in wavelength-independent fiber resonators. These results may also enable new opportunities for microresonator and bulk enhancement cavity platforms.

University of Rochester, University of Rochester Technology Development Fund, National Institutes of Health (NIH) (EB028933).

*xdong18@ur.rochester.edu

[1] S. A. Diddams, J. Opt. Soc. Am. B **27**, B51 (2010).
[2] T. J. Kippenberg, R. Holzwarth, and S. A. Diddams, Science **332**, 555 (2011).
[3] M.-G. Suh, Q.-F. Yang, K. Y. Yang, X. Yi, and K. J. Vahala, Science **354**, 600 (2016).
[4] D. T. Spencer, S. H. Lee, D. Y. Oh, M.-G. Suh, K. Y. Yang, and K. Vahala, Nature (London) **557**, 81 (2018).
[5] T. Udem, R. Holzwarth, and T. W. Hänsch, Nature (London) **416**, 233 (2002).
[6] P. Del'Haye, A. Schliesser, O. Arcizet, T. Wilken, R. Holzwarth, and T. J. Kippenberg, Nature (London) **450**, 1214 (2007).
[7] T. Steinmetz, T. Wilken, C. Araujo-Hauck, R. Holzwarth, T. W. Hänsch, L. Pasquini, A. Manescau, S. D'Odorico, M. T. Murphy, T. Kentischer, W. Schmidt, and T. Udem, Science **321**, 1335 (2008).
[8] P. Trocha, M. Karpov, D. Ganin, M. H. P. Pfeiffer, A. Kordts, S. Wolf, J. Krockenberger, P. Marin-Palomo, C. Weimann, S. Randel, W. Freude, T. J. Kippenberg, and C. Koos, Science **359**, 887 (2018).
[9] T. Herr, V. Brasch, J. D. Jost, C. Y. Wang, N. M. Kondratiev, M. L. Gorodetsky, and T. J. Kippenberg, Nat. Photonics **8**, 145 (2014).
[10] A. L. Gaeta, M. Lipson, and T. J. Kippenberg, Nat. Photonics **13**, 158 (2019).
[11] Y. Okawachi, K. Saha, J. S. Levy, Y. H. Wen, M. Lipson, and A. L. Gaeta, Opt. Lett. **36**, 3398 (2011).
[12] P. Del'Haye, T. Herr, E. Gavartin, M. L. Gorodetsky, R. Holzwarth, and T. J. Kippenberg, Phys. Rev. Lett. **107**, 063901 (2011).
[13] Y. K. Chembo and N. Yu, Opt. Lett. **35**, 2696 (2010).
[14] N. Lilienfein, C. Hofer, M. Högner, T. Saule, M. Trubetskov, V. Pervak, E. Fill, C. Riek, A. Leitenstorfer, J. Limpert, F. Krausz, and I. Pupeza, Nat. Photonics **13**, 214 (2019).
[15] F. Leo, S. Coen, P. Kockaert, S. P. Gorza, P. Emplit, and M. Haelterman, Nat. Photonics **4**, 471 (2010).
[16] J. K. Jang, M. Erkintalo, J. Schröder, B. J. Eggleton, S. G. Murdoch, and S. Coen, Opt. Lett. **41**, 4526 (2016).
[17] J. K. Jang, M. Erkintalo, S. G. Murdoch, and S. Coen, Nat. Photonics **7**, 657 (2013).
[18] M. Anderson, F. Leo, S. Coen, M. Erkintalo, and S. G. Murdoch, Optica **3**, 1071 (2016).
[19] J. K. Jang, M. Erkintalo, S. Coen, and S. G. Murdoch, Nat. Commun. **6**, 7370 (2015).
[20] W. H. Renninger and P. T. Rakich, Sci. Rep. **6**, 24742 (2016).
[21] L. F. Mollenauer and R. H. Stolen, Opt. Lett. **9**, 13 (1984).
[22] L. A. Lugiato and R. Lefever, Phys. Rev. Lett. **58**, 2209 (1987).
[23] C. Godey, I. V. Balakireva, A. Coillet, and Y. K. Chembo, Phys. Rev. A **89**, 063814 (2014).
[24] U. Morgner, S. H. Cho, H. A. Haus, E. P. Ippen, J. G. Fujimoto, Y. Chen, and F. X. Ka, J. Opt. Soc. Am. B **16**, 1999 (1999).
[25] K. Tamura, E. P. Ippen, H. A. Haus, and L. E. Nelson, Opt. Lett. **18**, 1080 (1993).
[26] M. Pawliszewska, T. Martynkien, A. Przewłoka, and J. Sotor, Opt. Lett. **43**, 38 (2018).
[27] S. K. Turitsyn, B. G. Bale, and M. P. Fedoruk, Phys. Rep. **521**, 135 (2012).
[28] C. Bao and C. Yang, Phys. Rev. A **92**, 023802 (2015).
[29] Y. Wang, F. Leo, J. Fatome, M. Erkintalo, S. G. Murdoch, and S. Coen, Optica **4**, 855 (2017).
[30] A. U. Nielsen, B. Garbin, S. Coen, S. G. Murdoch, and M. Erkintalo, APL Photonics **3**, 120804 (2018).
[31] See Supplemental Material at http://link.aps.org/supplemental/10.1103/PhysRevLett.125.033902 for further description of numerical simulations and experimental techniques.
[32] M. Malinowski, A. Rao, P. Delfyett, and S. Fathpour, APL Photonics **2**, 066101 (2017).
[33] E. Obrzud, S. Lecomte, and T. Herr, Nat. Photonics **11**, 600 (2017).
[34] Y. Wang, M. Anderson, S. Coen, S. G. Murdoch, and M. Erkintalo, Phys. Rev. Lett. **120**, 053902 (2018).